A Low Profile Dual-Band Dual-Polarized Filtering Antenna with No Extra Circuit

Xuekang Liu[1], Benito Sanz-Izquierdo[1], Steven Gao[2]
[1] (University of Kent): School of Engineering, Canterbury, UK, xl255@kent.ac.uk
[2] (Chinese University of Hong Kong): Department of Electronic Engineering, Hong Kong, China

Abstract*—This research introduces an innovative, compact dual-band dual-polarized antenna equipped with filtering capabilities for 5G sub-6GHz base stations. Using the concept of multipath coupling, two controllable radiation nulls are achieved independently. The antenna's impedance bandwidth is widened by skillfully exciting the anti-phase TM_{22} mode and shifting it to a lower frequency band while preserving other resonant modes. Additionally, incorporating four shorted strips around the radiator effectively increases the average half power beamwidth in the higher frequency band from 51° to 61°. Finally, the integration of two wide-band planar baluns, linked to the input terminals of the differentially fed antenna, results in the creation of this dual-polarized filtering antenna with dual operating frequency bands. Experimental prototypes of the antenna element and 1×4 array were fabricated and tested. The reflection coefficients demonstrate the antenna's functionality across the 3.24-3.90 GHz (18.5%) and 4.74-5.06 GHz (6.5%) frequency bands, maintaining $|S_{11}| < -14$ dB. Additionally, a high isolation level of 31 dB was measured from the input ports.

***Index Terms*— Base station array, dual-polarization, filtering antenna, dual-band array**

I. INTRODUCTION

Over the past few years, there has been global fascination and widespread attention directed towards fifth generation (5G) mobile communication systems. Many countries have announced their allocated/targeted 5G spectrum. Some of them (United Kingdom, Germany, Italy, etc.) have licensed one single band in sub-6GHz, while others (China, U.S., etc) have licensed two bands [1]. Many novel antennas were proposed in [2]-[6] to cover one of these targeted frequency bands. However, their single band characteristic is not enough for the increasingly integrated base station system. To achieve more comprehensive band coverage within the limited space, multi-band antennas have become a hot research topic in the field of antenna design, especially in base station antenna design. Besides possessing multi-band capabilities, an essential attribute for base station antennas is their filtering performance, crucial in mitigating mutual coupling with neighboring antennas. Therefore, the key task is to design a dual-polarized antenna that integrates both dual-frequency and filtering characteristics for base station systems.

To introduce radiation nulls, some new methods are presented in [7]-[9]. Defected ground structures (DGSs) were used in [8] to realize a radiation null in lower out-of-band. Effective improvement in the roll-off rate at the lower band edge was accomplished by symmetrically incorporating split-ring-shaped slots on the ground plane. A recently designed dual-band filtering antenna, as detailed in [9], exhibits a commendable out-of-band rejection level. This antenna effectively spans two broad frequency bands, ranging from 3.23-3.85 GHz and 5.29-5.74 GHz, while maintaining $|S_{dd11}| < -10$ dB. Its notable out-of-band rejection performance was achieved through a combination of DGS and differential feedlines. However, its single polarization characteristic limits its application in nowadays base station.

An antenna with dual-band and dual-polarization capabilities, spanning frequencies of 3.3-3.8 GHz and 4.8-5.0 GHz, was introduced in [10] by using novel double-oval-shaped feeding lines. However, this antenna does not have the ability to suppress unwanted signals. Through the utilization of resonator loaded with dual-mode stubs, a dual-band dual-polarized filtering antenna with second-order filtering characteristics was realized in [11]. The antenna achieves a compact size measuring $0.25\lambda_L \times 0.25\lambda_L \times 0.06\lambda_L$. However, the isolation between the two ports stands at a mere 20 dB. In [12], a dual-polarized patch antenna achieved two bandwidths (3.27-3.71 GHz and 4.8-5.18 GHz) and good filter response by combining slots and open circuit stepped-impedance resonators.

This paper introduces a novel dual-operating band filtering antenna for 5G base stations. It features dual-polarization, a compact size, high isolation, and exceptional out-of-band rejection levels. Measurement results align closely with simulated data. all of which were obtained through Ansys HFSS software simulations.

II. DUAL-BAND DUAL-POLARIZED FILTERING ELEMENT

Fig. 1 illustrates the geometry of the proposed dual-band dual-polarized filtering antenna (DBDPFA) element. The proposed antenna consists of a three-layer radiator, four shorted strips, a ground plane, and two feeding networks. The entirety of these structures is printed on Rogers 4003 substrates with different thicknesses (0.305mm: substrate 1&2; 0.813mm: substrate 3). The radiator can be divided into three metal layers. The first part is the parasitic polygon ring positioned on the upper surface of Sub 1. The second part is the slot loaded patch on the bottom of the sub 1. The third part

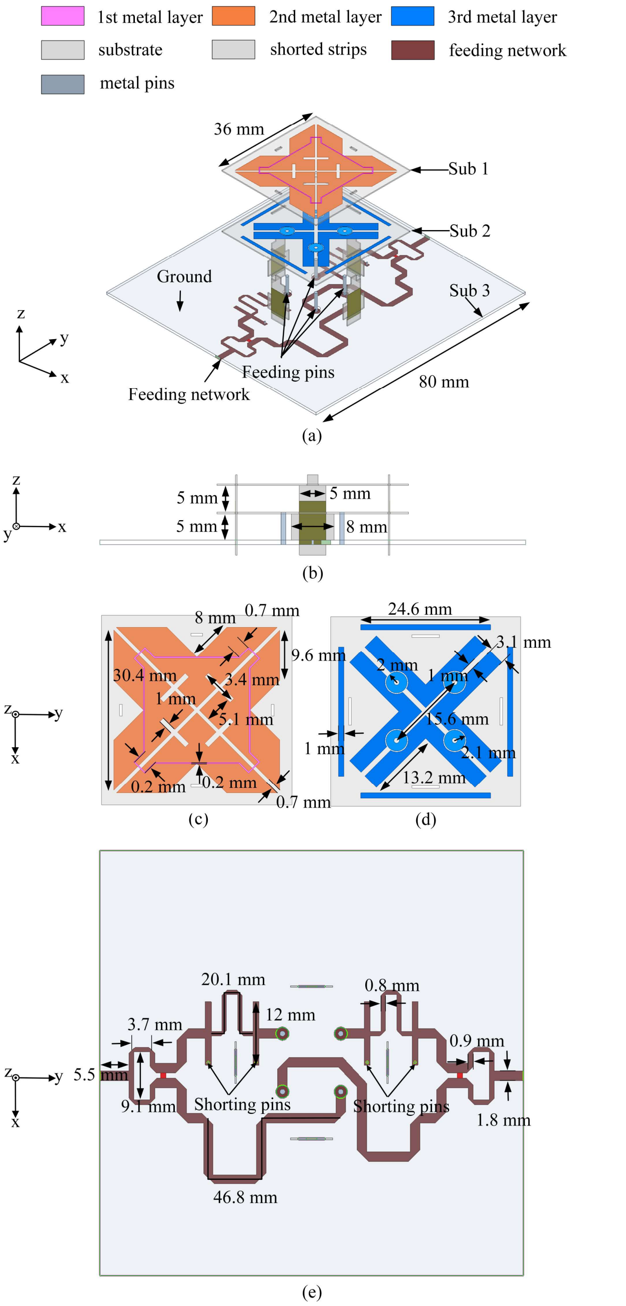

Fig. 1. DBDPFA's geometry. (a) exploded view, (b) lateral view, (c) upper perspective of Sub 1, (d) upper perspective of sub 2, and (e) feeding network.

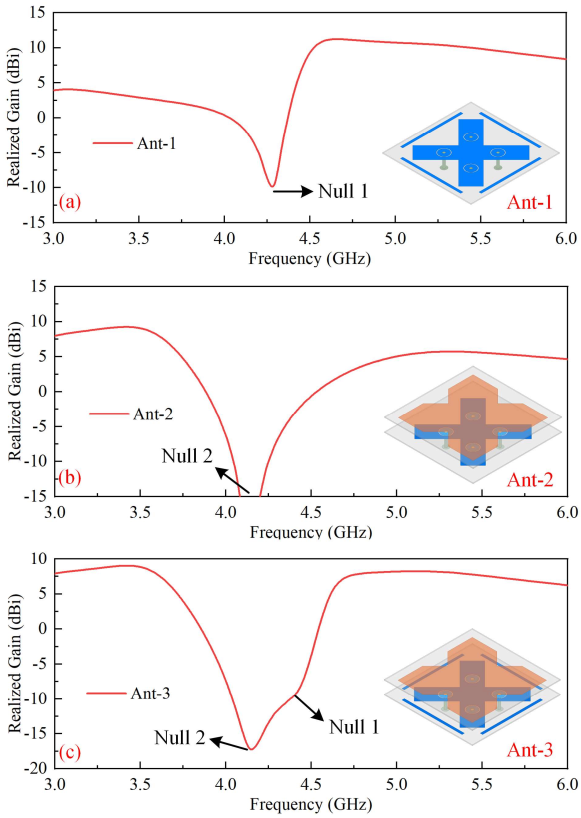

Fig. 2. Simulated results (realized gains in boresight direction) of the reference antennas. (a) Ant-1, (b) Ant-2, and (c) Ant-3.

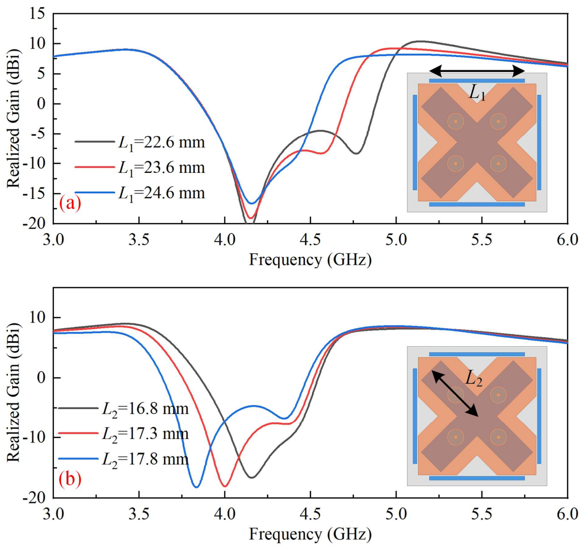

Fig. 3. Simulated results (realized gains in boresight direction) of the Ant-3 under different (a) L_1, and (b) L_2.

are the slot loaded crossed driven strip and parasitic linear strips positioned on the upper surface of Sub 2. Fig. 1 (b), (c), and (d) outline the specific dimensions of these components, while Fig. 1(e) presents the intricate design parameters of the feeding networks.

A. Radiation Nulls

For a more effective demonstration of the radiation nulls' working principles, Ant-1, Ant-2, and Ant-3 are developed. As givenin Fig. 2, Ant-1 consists of four parasitic linear strips and a crossed driven strip. Ant-2 consists of a crossed driven strip and a parasitic patch. The Ant-3 can be seen as a combination of Ant-1 and Ant-2. It's apparent that Ant-1 achieves a radiation null around 4.25 GHz, while Ant-2's radiation null emerges at approximately 4.15 GHz. Then, combining these two antennas enables the creation of a filtering antenna with two radiation nulls. Both radiation nulls are realized by using the principle of multipath coupling [13].

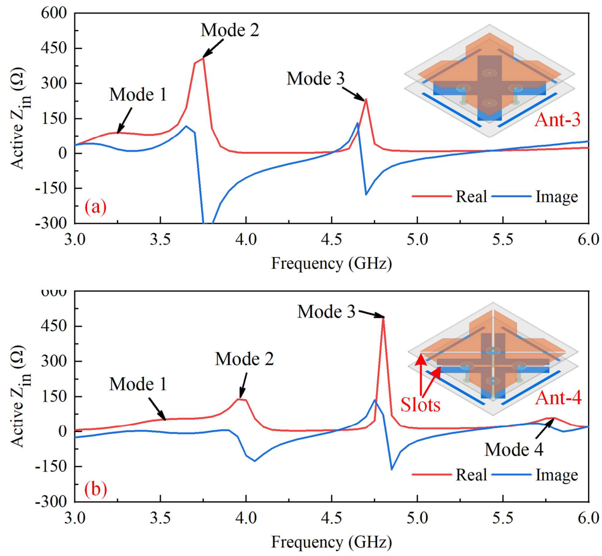

Fig. 4. Simulated input impedance of the (a) Ant-3 and (b) Ant-4.

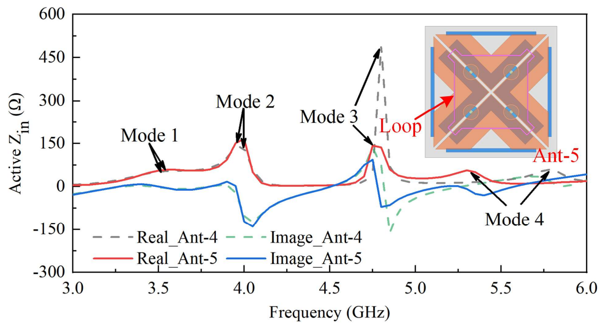

Fig. 5. Simulated input impedance of Ant-4 and Ant-5.

For a more profound understanding of the radiation nulls' functioning, two key parameters (L_1 and L_2) are chosen to do the parameter study. Fig. 3(a) and (b) show the simulated realized gain of the Ant-3 in boresight direction under different L_1 and L_2. It can be clearly seen that both radiation nulls can be adjusted independently. The final values of these two parameters can be determined according to our requirements for specific antenna design. L_1=24.6 mm and L_2=16.8 mm are chosen in our design.

B. Excitation and Shift of Anti-Phase TM_{22} Mode

The relatively narrow bandwidth has been a major drawback of microstrip patch antenna. To overcome this problem, the method of merging multiple resonant modes [14], [15] has been widely noticed because it does not increase either the antenna aperture or the antenna profile. In this sub-section, a new resonant mode named anti-phase TM_{22} mode will be excited and manipulated to improve the proposed antenna's impedance bandwidth.

Fig.4 shows the input impedance of the Ant-3 and Ant-4 Three resonant mode entitled mode 1 (TM_{10} mode of the parasitic patch), mode 2 (TM_{10} mode of the crossed driven strip), and mode 3 (resonant mode of the parasitic strips) are

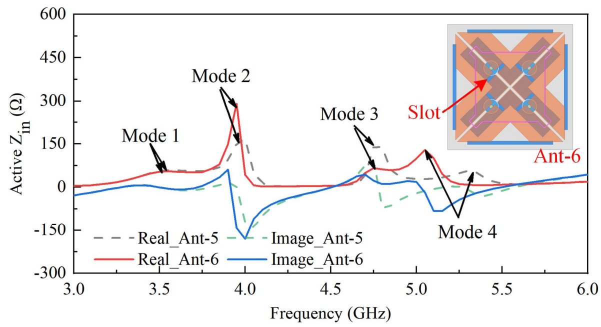

Fig. 6. Simulated input impedance of the Ant-5 and Ant-6.

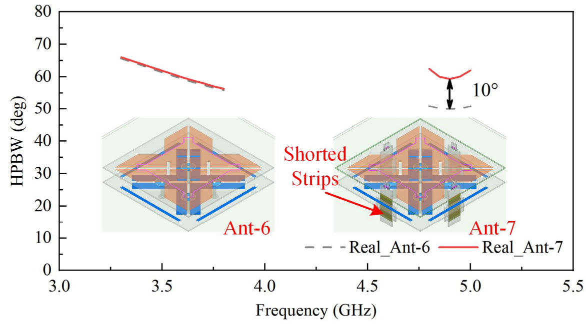

Fig. 7. Simulated HPBW of the Ant-6 and Ant-7.

excited to cover the target frequency ranges (3.3-3.8 GHz and 4.8-5.0 GHz). The lower band (LB) can be covered by mode 1 and 2. However, only mode 3 is not enough to cover the higher band (HB). Therefore, a new resonant mode should be excited without suppression on the existing resonant modes. As depicted in Fig. 4(b), introducing slots on both the crossed driven strip and parasitic patch creates a new resonant mode, further enhancing the impedance bandwidth.

Although a new resonant appears at 5.75 GHz, the frequency ratio (FR) between the mode 3 and this new mode is too large, hindering the formation of a broad impedance bandwidth. To reduce the FR, a parasitic polygon ring is printed above the slot-loaded parasitic patch. As depicted in Fig. 5, after introducing the polygon ring, the resonant frequency of the anti-phase TM_{22} mode is shift from 5.75 GHz to 5.30 GHz. The FR is reduced from 1.21 to 1.11.

To further reduce the FR, more slots are etched on parasitic patch. After introducing the slots, the effective current path of the anti-phase TM_{22} mode can be extended. Hence, the resonant frequency can be shifted towards a lower frequency band. As depicted in Fig. 6, employing this technique can decrease the FR to 1.06.

C. Results and Discussion

For a base station antenna, the half power beamwidth (HPBW) is also a crucial metric except filtering performance and impedance bandwidth. Fig. 7 illustrates that the presented antenna's average HPBW in the HB can be significantly increased from 51° to approximately 61°. This enhancement occurs without impacting the HPBW in the LB by

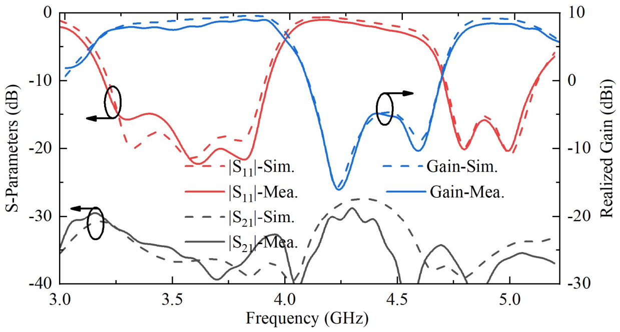

Fig. 8. Experimental and simulated S-parameters, along with the realized gain of the antenna element.

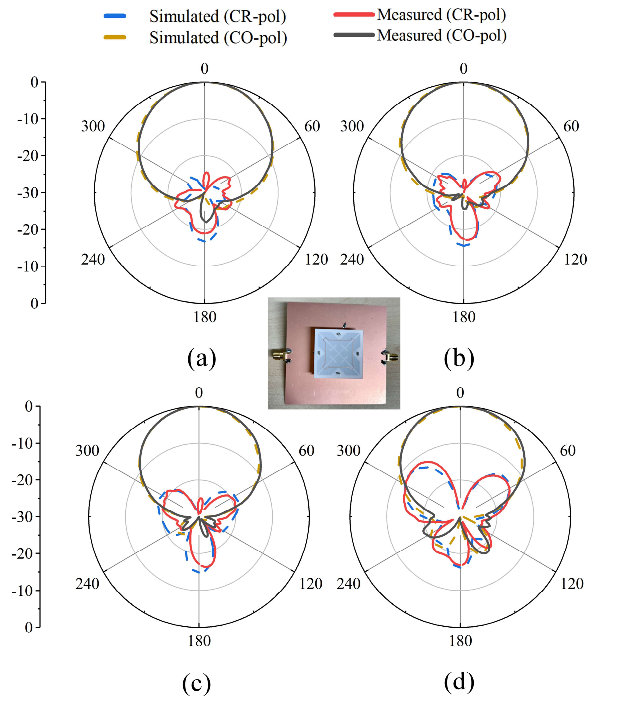

Fig. 9. Experimental and simulated normalized radiation patterns of the presented antenna element in horizontal plane at (a) 3.3 GHz, (b) 3.6 GHz, (c) 3.8 GHz, and (d) 4.9 GHz.

symmetrically introducing four shorted strips around the antenna. Finally, two feeding networks are introduced to minimize the number of input ports from four to two for ease of measurement.

The findings illustrated in Fig. 8 demonstrate that this antenna element efficiently functions in two separate frequency ranges: 3.24-3.90 GHz and 4.74-5.06 GHz. The isolation between the differential ports exceeds 31 dB. At broadside, the maximum measured realized gain reaches 9.2 dBi and 8.8 dBi for the LB and HB. Fig. 9 illustrates the stability of the radiation patterns within these operational frequency ranges. The HPBWs are approximately 62°. Moreover, the measured cross-polarization levels demonstrate a 25 dB reduction compared to the co-polarization level.

Table I presents a comparison of the essential characteristics between our design and the designs presented in other papers. This analysis reveals that the antenna introduced in this paper holds promising prospects for utilization within 5G base station systems.

TABLE I
COMPARISON BETWEEN FILTERING ANTENNAS

Ref.	Polar.	Imp. BW	Size (λ_L)	NP	HPBW
[9]	Single	*3.23-3.85 (17.5%) *5.29-5.74 (8.2%)	0.42×0.28× 0.06	2	/
[11]	0°; 90°	*5.1-5.3 (3.8%) *9.6-10.2 (6.1%)	0.25×0.25× 0.06	2	/
[12]	±45°	3.28-3.71 (12.3%) 4.8-5.18 (7.6%)	0.42×0.42× 0.12	4	65° 52°
Pro.	±45°	**3.24-3.90 (18.5%)** **4.74-5.06 (6.5%)**	**0.36×0.36×** **0.12**	**2**	**63°** **62°**

* means the reference level of $|S_{11}|$ is -10 dB, NP represents number of ports.

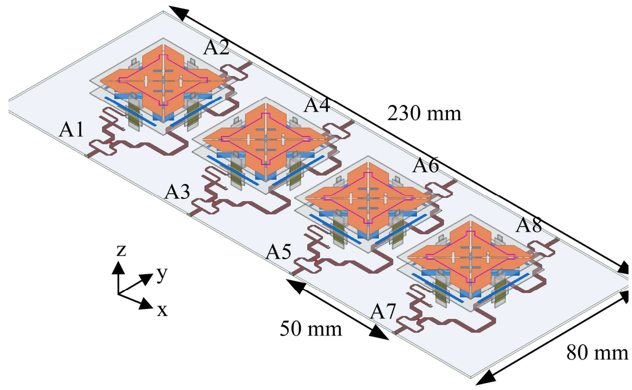

Fig. 10. Configuration of the presented array antenna.

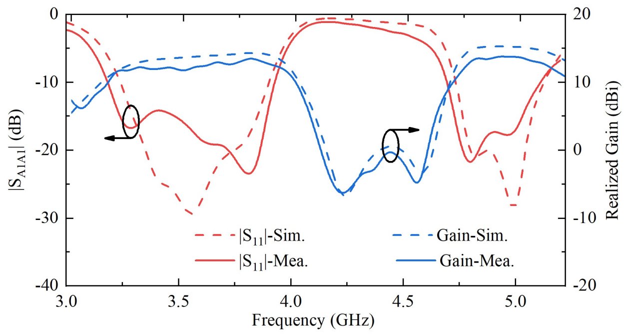

Fig. 11. Measured and simulated $|S_{11}|$ and realized gain of the presented array antenna.

III. DUAL-BAND DUAL-POLARIZED FILTERING ARRAY

Utilizing the presented antenna element as a foundation, a dual-polarized filtering array antenna with dual operating frequency ranges has been developed. As illustrated in Fig. 10, the proposed array antenna has a ground size of 230 mm × 80mm. The spacing between the antenna elements is 50 mm, equivalent to 0.54λ at the lowest frequency.

Fig. 11 depicts the simulated and tested $|S_{11}|$ of the array antenna. The measurements indicate that the proposed array effectively spans 3.23-3.9 GHz and 4.72-5.05 GHz, maintaining a reference level of $|S_{11}| < -14$ dB. Notably, the maximum measured realized gains reach approximately 13.7 dB and 13.8 dB in the LB and HB, respectively.

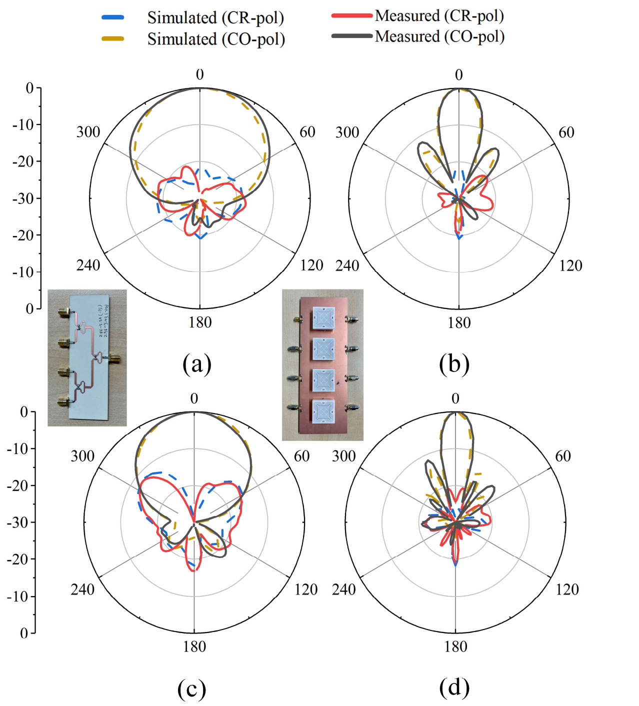

Fig. 12. Normalized radiation patterns of the array antenna in horizontal plane (a) 3.6 GHz, (c) 4.9 GHz and vertical plane (b) 3.6 GHz, (d) 4.9 GHz.

Fig. 12 presents the normalized radiation patterns of the array antenna in both planes (horizontal and vertical) at center frequencies of the two operational frequency bands. Only the radiation patterns for one of the polarizations are shown here due to the symmetry. The consistency between the measured and the simulated results is notable. Minor variations in cross-polarization can be attributed to spurious radiation emanating from the connectors and cables. At 3.6 GHz, the HPBW in horizontal plane is 64°, while its counterpart in vertical plane is 20°. At 4.9 GHz, HPBWs of 55° and 15° are achieved in horizontal and vertical plane, respectively.

IV. Conclusion

This paper introduces the design of a new low profile DBDPFA. Through the application of multipath coupling principles, two radiation nulls are strategically incorporated between the two operational frequency bands to effectively mitigate unwanted radiation. Furthermore, anti-phase TM_{22} mode is utilized for the first time in this paper to enhance impedance bandwidth of dual-polarized antenna. By symmetrically introducing shorted strips around the radiator, the HPBW of the proposed antenna at HB can be significantly improved by 10°. The measured outcomes of both the antenna element and the 1×4 array align well with the simulated data. These results affirm that the proposed antenna element and array effectively span the designated 5G spectrum in various countries, including the European Union, UK, Germany, China, and others. A dual-polarized filtering antenna with dual working frequency bands and such a low profile is a strong contender for 5G base-station applications.

Acknowledgment

Partial support for this project was provided by Huawei Technologies Ltd, and additional funding was received from EPSRC under Grants EP/S005625/1 and EP/N032497/1.

References

[1] Global update on spectrum for 4G & 5G. Accessed: Dec. 2020. [online]. Available:https://www.qualcomm.com/content/dam/qcomm-martech/dm-assets/documents/messaging_presentation_-_4g_5g_spectrums_-_december_2020.pdf.

[2] K. Xue, D. Yang, C. Guo, H. Zhai, H. Li, and Y. Zeng, “A dual-polarized filtering base-station antenna with compact size for 5G applications,” IEEE Antennas Wireless Propag. Lett., vol. 19, no. 8, pp. 1316-1320, Aug. 2020.

[3] H. Huang, X. Li, and Y. Liu, “A low-profile, single-ended and dual-polarized patch antenna for 5G application,” IEEE Trans. Antennas Propag., vol. 68, no. 5, pp. 4048-4053, May 2020.

[4] X. Liu et al., “A mutual-coupling-suppressed dual-band dual-polarized base station antenna using multiple folded-dipole antenna,” IEEE Trans. Antennas Propag., vol. 70, no. 12, pp. 11582-11594, Dec. 2022.

[5] S. Liu, Z. Wang, and Y. Dong, “Compact wideband SRR-inspired antennas for 5G microcell applications,” IEEE Trans. Antennas Propag., vol. 69, no. 9, pp. 5998-6003, Sept. 2021.

[6] M. Li, X. Chen, A. Zhang, and A. A. Kishk, “Dual-polarized broadband base station antenna backed with dielectric cavity for 5G communications,” IEEE Antennas Wireless Propag. Lett., vol. 18, no. 10, pp. 2051-2055, Oct. 2019.

[7] X. Liu et al., “A compact dual-polarized filtering antenna with steep cut-off for base-station applications,” IEEE Trans. Antennas Propag., vol. 70, no. 7, pp. 5941-5946, July 2022.

[8] W. Yang, M. Xun, W. Che, W. Feng, Y. Zhang, and Q. Xue, “Novel compact high-gain differential-fed dual-polarized filtering patch antenna,” IEEE Trans. Antennas Propag., vol. 67, no. 12, pp. 7261-7271, Dec. 2019.

[9] D. Li, M. -C. Tang, Y. Wang, K. -Z. Hu, and R. W. Ziolkowski, “Dual-band, differentially-fed filtenna with wide bandwidth, high selectivity, and low cross-polarization,” IEEE Trans. Antennas Propag., vol. 70, no. 6, pp. 4872-4877, June 2022.

[10] Q. Hua, Y. Huang, A. Alieldin, C. Song, T. Jia, and X. Zhu, “A dual-band dual-polarized base station antenna using a novel feeding structure for 5G communications,” IEEE Access, vol. 8, pp. 63710-63717, 2020.

[11] C. -X. Mao, S. Gao, Y. Wang, Q. Luo, and Q. -X. Chu, “A shared-aperture dual-band dual-polarized filtering-antenna-array with improved frequency response,” IEEE Trans. Antennas Propag., vol. 65, no. 4, pp. 1836-1844, April 2017.

[12] Y. Li, Z. Zhao, Z. Tang, and Y. Yin, “Differentially fed, dual-band dual-polarized filtering antenna with high selectivity for 5G Sub-6 GHz base station applications,” IEEE Trans. Antennas Propag., vol. 68, no. 4, pp. 3231-3236, April 2020.

[13] J. B. Thomas, “Cross-coupling in coaxial cavity filters - a tutorial overview,” IEEE Trans. Microw. Theory Techn., vol. 51, no. 4, pp. 1368-1376, April 2003.

[14] X. Liu et al., “A wideband triple-mode differentially fed microstrip patch antenna,” IEEE Antennas Wireless Propag. Lett., vol. 20, no. 7, pp. 1160-1164, July 2021.

[15] N. -W. Liu, L. Zhu, W. -W. Choi and X. Zhang, “A low-profile aperture-coupled microstrip antenna with enhanced bandwidth under dual resonance,” IEEE Trans. Antennas Propag., vol. 65, no. 3, pp. 1055-1062, March 2017.